

Catalysis Science & Technology

Accepted Manuscript



This is an *Accepted Manuscript*, which has been through the Royal Society of Chemistry peer review process and has been accepted for publication.

Accepted Manuscripts are published online shortly after acceptance, before technical editing, formatting and proof reading. Using this free service, authors can make their results available to the community, in citable form, before we publish the edited article. We will replace this *Accepted Manuscript* with the edited and formatted *Advance Article* as soon as it is available.

You can find more information about *Accepted Manuscripts* in the [Information for Authors](#).

Please note that technical editing may introduce minor changes to the text and/or graphics, which may alter content. The journal's standard [Terms & Conditions](#) and the [Ethical guidelines](#) still apply. In no event shall the Royal Society of Chemistry be held responsible for any errors or omissions in this *Accepted Manuscript* or any consequences arising from the use of any information it contains.

Submitted to *Catal. Sci. Technol.* as an Article (revised)

Synthesis and oxidation catalysis of a Ti-substituted phosphotungstate, and identification of the active oxygen species

Eri Takahashi,^a Keigo Kamata,^{a,b} Yuji Kikukawa,^{a,c} Sota Sato,^d Kosuke Suzuki,^a Kazuya Yamaguchi,^a and Noritaka Mizuno^{*a}

^aDepartment of Applied Chemistry, School of Engineering, The University of Tokyo, 7-3-1 Hongo, Bunkyo-ku, Tokyo 113-8656, Japan

^bPresent Address: Materials and Structures Laboratory, Tokyo Institute of Technology, Nagatsuta-cho 4259, Midori-ku, Yokohama-city, Kanagawa 226-8503, Japan

^cPresent Address: Department of Chemistry, Division of Material Sciences, Graduate School of Natural Science and Technology, Kanazawa University, Kakuma-machi, Kanazawa 920-1192, Japan

^dJST, ERATO, Isobe Degenerate π -Integration Project, Aoba-ku, Sendai 980-8577, Japan; Advanced Institute for Materials Research (AIMR) and Department of Chemistry, Tohoku University, Aoba-ku, Sendai 980-8578, Japan

Abstract

In this paper, we report the synthesis of a Ti-substituted phosphotungstate, $\text{TBA}_6[(\gamma\text{-PW}_{10}\text{O}_{36})_2\text{Ti}_4(\mu\text{-O})_2(\mu\text{-OH})_4]$ (**I**, TBA = tetra-*n*-butylammonium), and its application to H_2O_2 -based oxidation. Firstly, an organic solvent-soluble dilacunary phosphotungstate precursor, $\text{TBA}_3[\gamma\text{-PW}_{10}\text{O}_{34}(\text{H}_2\text{O})_2]$ (PW10), has been synthesized. By the reaction of PW10 and $\text{TiO}(\text{acac})_2$ (acac = acetylacetonate) in an organic medium (acetonitrile), **I** can be obtained. Compound **I** possesses a tetranuclear Ti core which can effectively activate H_2O_2 and show high catalytic performance for several oxidation reactions, such as epoxidation of alkenes, oxygenation of sulfides, oxidative bromination of unsaturated compounds, and the hydroxylation of anisole, giving the corresponding oxidation products with high efficiencies and selectivities. The catalytic performance of **I** is much superior to those of the previously reported Ti-substituted polyoxometalates. In addition, **I** is highly durable during the catalysis and can be reused several times with keeping its high catalytic performance. Furthermore, we have successfully isolated the truly catalytically active species for the present **I**-catalyzed oxidation, $\text{TBA}_6[(\gamma\text{-PW}_{10}\text{O}_{36})_2\text{Ti}_4(\mu\text{-}\eta^2\text{:}\eta^2\text{-O}_2)_4]$ (**II**), and its anion structure has been determined by X-ray crystallographic analysis. All of the four $\text{Ti}_2\text{-}\mu\text{-}\eta^2\text{:}\eta^2\text{-peroxo}$ species in **II** are active for stoichiometric oxidation (without H_2O_2), and **II** is included in the catalytic cycle for the **I**-catalyzed oxidation.

Submitted to *Catal. Sci. Technol.* as an Article (revised)

Introduction

Selective oxidation is one of the most prevalent transformations in a broad range of fields, and the oxygenated products, such as epoxides, alcohols, aldehydes, ketones, and carboxylic acids, greatly contribute to the quality of our lives. However, oxidation processes sometimes lead to vast amounts of wastes; for example, dichromate, permanganate, and peracids are still frequently utilized in (super)stoichiometric amounts especially for fine chemicals production. In order to minimize wastes in the laboratory-scale as well as the industrial-scale productions, the antiquated stoichiometric oxidation processes should be replaced with catalytic ones.¹ The choice of oxidants is also very important, and H₂O₂ and O₂ (or air) are regarded as “greener oxidants” because of their high contents of active oxygen species, e.g., 47 wt% in the case of H₂O₂, and co-production of only water.¹ Therefore, the current most important subject of basic researches is to develop reliable catalysts that can activate the greener oxidants and transfer the active oxygen species to various substrates with high efficiency and selectivity.

Up to the present, a number of transition-metal catalysts have been developed for H₂O₂-based oxidation of various substrates.^{2–10} The activation of H₂O₂ by transition-metal catalysts typically proceeds through one-electron (Fenton-like) mechanism, two-electron mechanism, or both.¹¹ Unlike one-electron mechanism, free-radical intermediates are not involved, competitive non-productive H₂O₂ decomposition are suppressed, and electrophilically activated metal-(hydro)peroxo and/or metal-oxo species are recognized to be formed in two-electron mechanism.¹¹ Thus, two-electron mechanism is desirable for H₂O₂-based selective oxidation especially for electrophilic oxygen transfer reactions to organic substrates. Generally, Ti, V, Mo, W, and Re in their d⁰ electronic configurations are the principal metals that can catalyze H₂O₂-based oxidation through two-electron mechanism.¹¹

Amongst d⁰-metal catalysts for H₂O₂-based oxidation, Ti-based catalysts have extensively been investigated.^{2–4} Since the first report on synthesis and oxidation catalysis of TS-1 (titanium silicalite-1),^{2a} numerous Ti-containing zeolites have been synthesized by isomorphous substitution

Submitted to *Catal. Sci. Technol.* as an Article (revised)

for Si (or Al) in the framework.² The tetrahedrally coordinated Ti site in TS-1 is believed to contribute the oxidation catalysis, and Ti(η^1 -OOH), Ti(η^2 -OOH), and/or Ti(η^2 -O₂) species (with coordination of an alcohol (solvent) or a water molecule to the Ti site) have been postulated as active oxygen species on the basis of both experimental approaches and computational calculations (Fig. 1a).^{2,12} Recently, Katsuki and co-workers have reported the synthesis of bis- μ -oxo Ti(salen) and Ti(salan) dimeric complexes and their utilization for enantioselective epoxidation with H₂O₂.^{3a,b} Soon after, they have successfully synthesized a μ -oxo- μ - η^2 : η^2 -peroxo Ti(salan) complex by the reaction of the bis- μ -oxo complex with H₂O₂, and its structure has been determined by X-ray crystallographic analysis.^{3c} Although the μ -oxo- μ - η^2 : η^2 -peroxo complex is effective for catalytic epoxidation with H₂O₂, it is completely inactive for stoichiometric epoxidation. Thus, the complex is not a truly catalytically active species but just a “precursor” of active species (Fig. 1b).^{3c} As stated above, although Ti catalysts are recognized to be effective for H₂O₂-based oxidation, the truly catalytically active species as well as the detailed reaction mechanism are still unclear and controversial.

We have engaged in design of polyoxometalate (POM)-based molecular catalysts for a long time.¹³ POMs are a large class of metal-oxygen cluster anions, and their properties, such as redox potentials, acidic and basic properties, and solubilities, can finely be tuned by choosing constituent elements and counter cations.¹⁴ In particular, POMs are attractive materials for oxidation catalysts because they are thermally and oxidatively stable, and active site structures can precisely be designed by using lacunary POMs as the “structural motifs”.¹⁴ To date, various kinds of metal-substituted POMs have been synthesized for H₂O₂-based oxidation.^{14,15} With regard to Ti-substituted ones, $[(\gamma\text{-SiW}_{10}\text{O}_{36})_2\text{Ti}_4(\mu\text{-O})_2(\mu\text{-OH})_4]^{8-}$,^{4a} $[\text{PW}_{11}\text{TiO}_{40}]^{5-}$,^{4b-d} $[\text{PW}_{10}\text{Ti}_2\text{O}_{40}]^{7-}$,^{4b} $[(\alpha\text{-}1,2,3\text{-PW}_9\text{Ti}_3\text{O}_{37})_2(\mu\text{-O})_3]^{12-}$,^{4e} $[\alpha\text{-PW}_{10}\{\text{Ti}(\text{O}_2)\}_2\text{O}_{38}]^{7-}$,^{4f} and $[(\text{B-}\alpha\text{-AsW}_9\text{O}_{33})_2\{\text{Ti}(\text{OH})\}_2\{\text{WO}(\text{H}_2\text{O})\}]^{8-}$ ^{4g} are the typical examples. Despite these advances, there is still plenty room for improvement in their catalytic activities, and in addition their truly catalytically active species have never been clarified and isolated. A POM with Ti-peroxo species,

Submitted to *Catal. Sci. Technol.* as an Article (revised)

$[\alpha\text{-}1,2,3\text{-P}_2\text{W}_{15}\text{O}_{56}\{\text{Ti}(\eta^2\text{-O}_2)\}_3(\mu\text{-OH})_3]^{9-}$, has also been synthesized but this peroxo species is too stable to oxidize substrates.¹⁶

In this study, we have synthesized for the first time a Ti-substituted phosphotungstate with a tetranuclear Ti core, $\text{TBA}_6[(\gamma\text{-PW}_{10}\text{O}_{36})_2\text{Ti}_4(\mu\text{-O})_2(\mu\text{-OH})_4]$ (**I**, TBA = tetra-*n*-butylammonium), by the reaction of an organic solvent-soluble divacant lacunary phosphotungstate, $\text{TBA}_3[\gamma\text{-PW}_{10}\text{O}_{34}(\text{H}_2\text{O})_2]$ (PW10), with an appropriate Ti^{4+} source ($\text{TiO}(\text{acac})_2$, acac = acetylacetonate) in acetonitrile (CH_3CN). Compound **I** could act as an efficient reusable catalyst for several H_2O_2 -based oxidation reactions, such as epoxidation of alkenes, oxygenation of sulfides, oxidative bromination of unsaturated compounds, and the hydroxylation of anisole. In addition, we have successfully isolated the truly catalytically active species, $\text{TBA}_6[(\gamma\text{-PW}_{10}\text{O}_{36})_2\text{Ti}_4(\mu\text{-}\eta^2\text{:}\eta^2\text{-O}_2)_4]$ (**II**), and its anion structure has been determined by X-ray crystallographic analysis (Fig. 1c).

Results and discussion

Synthesis and structural characterization of a titanium-substituted phosphotungstate

Generally, the introduction of metal cations into the vacant sites of lacunary POMs has been performed in aqueous media, and various metal-substituted POMs with unique structures and properties have been synthesized.^{13–15} However, the synthesis in aqueous media should require strict control of the synthetic conditions, such as pH, temperature, and concentration, and POMs frequently isomerized to unexpected structures.¹⁷ In addition, alkali metal cations (counter cations) strongly coordinate to the vacant sites of lacunary POMs, which frequently inhibit the introduction of metal cations into the vacant sites.¹⁸ We have recently utilized organic solvent-soluble lacunary POMs, e.g., $\text{TBA}_4[\gamma\text{-SiW}_{10}\text{O}_{34}(\text{H}_2\text{O})_2]$ (SiW10),^{8a} as the precursors and introduced metal cations into their lacunary pockets in organic media.¹⁹ In the synthesis in organic media, the undesirable isomerization of lacunary precursors can be avoided during the metal introduction. We have recently found that the reactivity of metal-substituted POMs with H_2O_2 can be increased by changing the central heteroatoms from Si^{4+} to P^{5+} , leading to the significant improvement of catalytic activities for

Submitted to *Catal. Sci. Technol.* as an Article (revised)

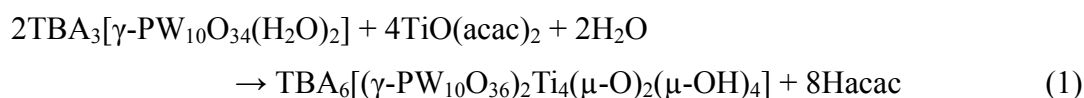
electrophilic oxidation; for example, the reaction rate of the epoxidation of allyl acetate by a V-substituted phosphotungstate, $[\gamma\text{-PW}_{10}\text{O}_{38}\text{V}_2(\mu\text{-OH})_2]^{3-}$, was ca. 16 times larger than that by the silicotungstate analogue $[\gamma\text{-SiW}_{10}\text{O}_{38}\text{V}_2(\mu\text{-OH})_2]^{4-}$.²⁰ However, until now there are only five examples (V, Mn, Mo, W, and Ru)²¹ of metal substitution into $[\gamma\text{-PW}_{10}\text{O}_{36}]^{7-}$ likely owing to the low stability and solubility of $[\gamma\text{-PW}_{10}\text{O}_{36}]^{7-}$ (typically Cs salt) in aqueous media.

In order to demonstrate the metal substitution in organic media, the organic solvent-soluble $[\gamma\text{-PW}_{10}\text{O}_{36}]^{7-}$ precursors (e.g., TBA salt) should be required, but they are unprecedented compounds. Therefore, we firstly attempted to synthesize an organic solvent-soluble divacant lacunary phosphotungstate precursor (PW10) by the cation exchange reaction of $\text{Cs}_7[\gamma\text{-PW}_{10}\text{O}_{36}]^{22}$ with TBABr. To avoid undesirable isomerization of the POM framework, the reaction was carefully carried out at low temperature (273 K). The IR spectrum of PW10 showed the bands around 1109–1036, 975–951, and 861–798 cm^{-1} assignable to $\nu(\text{P-O})$, $\nu(\text{W=O})$, and $\nu(\text{W-O-W})$, respectively, and these bands were also observed at the similar regions in the case of $\text{Cs}_7[\gamma\text{-PW}_{10}\text{O}_{36}]$ (Fig. S1a,b). The ^{31}P NMR spectrum of PW10 in $\text{DMSO-}d_6$ showed a single signal at -10.5 ppm (Fig. 2a). The ^{183}W NMR spectrum of PW10 in $\text{DMSO-}d_6$ showed five signals at -105.4 , -114.2 , -117.3 , -136.1 , and -168.5 ppm with the respective intensity ratio of 1:1:1:1:1, indicating that PW10 possesses the C_2 symmetry in the solution-state which is the same as that of the silicotungstate analogue SiW10 (Fig. 3a).^{8a} The cold-spray ionization mass (CSI-MS) spectrum of PW10 in acetone showed the signal set at $m/z = 3384$ with the isotopic distribution which agreed with the pattern calculated for $[\text{TBA}_4(\text{PW}_{10}\text{O}_{34})]^+$ (Fig. S2a). The elemental analysis data showed the TBA/P/W ratio of 3:1:10. Therefore, the formula of PW10 is possibly $\text{TBA}_3[\gamma\text{-PW}_{10}\text{O}_{34}(\text{H}_2\text{O})_2]$.

By using PW10 as the precursor, a Ti-substituted phosphotungstate (**I**) could successfully be synthesized. Compound **I** could readily be synthesized by just simply mixing the required components of PW10 and a suitable Ti source ($\text{TiO}(\text{acac})_2$, two equivalents with respect to PW10) in CH_3CN at room temperature. Fortunately, the single crystals of **I** suitable for X-ray crystallographic analysis were obtained by recrystallization from a mixed solvent of CH_3CN and ethyl acetate

Submitted to *Catal. Sci. Technol.* as an Article (revised)

(EtOAc), and its structure was successfully determined. The structure of the anion part of **I** is shown in Fig. 4, and the crystallographic data are summarized in Table S1. An edge-shared oxygen-bridged dinuclear titanium core was introduced into the lacunary pocket of $[\gamma\text{-PW}_{10}\text{O}_{36}]^{7-}$, and two monomer subunits were linked by two Ti–O–Ti fragments. Six TBA cations per **I** anion could crystallographically be assigned in accord with the elemental analysis data. The bond valence sum (BVS) values of phosphorus (4.96), tungsten (5.98–6.15), and titanium (4.22–4.24) atoms in **I** indicate that the respective valences are +5, +6, and +4. Therefore, four protons are associated with **I** anion. The BVS values of O1a and O1b were 1.23 and 1.27, respectively, suggesting that these oxygens are monoprotonated to form the $[\text{Ti}_2(\mu\text{-OH})_2]^{6+}$ core in the subunit. The BVS value of O1c was 2.10, showing that the bridging oxygen atom is $\mu\text{-O}$ species. The X-ray crystallographic and elemental analysis data show that the formula of **I** is $\text{TBA}_6[(\gamma\text{-PW}_{10}\text{O}_{36})_2\text{Ti}_4(\mu\text{-O})_2(\mu\text{-OH})_4]$. The formation of **I** can be expressed by the following equation [eqn (1)].



The anion structure of **I** was intrinsically isostructural with those of the previously reported $\text{TBA}_8[(\gamma\text{-SiW}_{10}\text{O}_{36})_2\text{Ti}_4(\mu\text{-O})_2(\mu\text{-OH})_4]^{4a}$ and $\text{K}_8[(\gamma\text{-GeW}_{10}\text{O}_{36})_2\text{Ti}_4(\mu\text{-O})_2(\mu\text{-OH})_4]^{23}$. The lengths of Ti···Ti (3.18–3.48 Å), Ti–OH (1.98–2.00 Å), and Ti–O (1.79–1.80 Å), and the angles of Ti–OH–Ti (105.58–106.58°) and Ti–O–Ti (151.09°) in **I** were quite similar to those in $\text{TBA}_8[(\gamma\text{-SiW}_{10}\text{O}_{36})_2\text{Ti}_4(\mu\text{-O})_2(\mu\text{-OH})_4]$ and $\text{K}_8[(\gamma\text{-GeW}_{10}\text{O}_{36})_2\text{Ti}_4(\mu\text{-O})_2(\mu\text{-OH})_4]$ (Table S2). By contrast, the lengths of Ti···P (3.77–3.79 Å) in **I** were slightly longer than those of Ti···Si (3.61–3.69 Å) in $\text{TBA}_8[(\gamma\text{-SiW}_{10}\text{O}_{36})_2\text{Ti}_4(\mu\text{-O})_2(\mu\text{-OH})_4]$ and Ti···Ge (3.60–3.61 Å) in $\text{K}_8[(\gamma\text{-GeW}_{10}\text{O}_{36})_2\text{Ti}_4(\mu\text{-O})_2(\mu\text{-OH})_4]$.

The ^{31}P NMR spectrum of **I** in CD_3CN showed a single signal at –11.8 ppm, indicating the presence of **I** as the single species (Fig. 2b). The ^1H NMR spectrum of **I** in CD_3CN showed signals assignable to TBA cations (1.01, 1.43, 1.67, and 3.17 ppm) and $\mu\text{-OH}$ species (7.91 ppm) (Fig. S3).

Submitted to *Catal. Sci. Technol.* as an Article (revised)

The ^{183}W NMR spectrum of **I** in a mixed solvent of CD_3CN and propylene carbonate (PC, 1:1 v/v) showed three signals at -110.6 , -112.7 , and -115.8 ppm with the respective intensity ratio of 1:2:2 in accord with the C_{2v} symmetry of **I** in the solid-state (Fig. 3b).²⁴ The CSI-MS spectrum of **I** in CH_3CN showed the two sets of signals centered at $m/z = 3561$ and 3674 assignable to $[\text{TBA}_8\text{H}_4\{(\text{PW}_{10}\text{O}_{36})_2\text{Ti}_4\text{O}_6\}]^{2+}$ and $[\text{TBA}_9\text{H}\{(\text{PW}_{10}\text{O}_{36})_2\text{Ti}_4\text{O}_5\}]^{2+}$, respectively (Fig. S2b). These NMR and CSI-MS spectra agreed well with the crystal structure of **I**, indicating that the solid-state structure of **I** is maintained in the solution-state.

Catalytic performance for H_2O_2 -based oxidations

To begin with, the epoxidation of cyclooctene with 30 % aqueous H_2O_2 was carried out as the test reaction (Table 1). Under the present reaction conditions, the epoxidation did not proceed at all in the absence of catalysts (Table 1, entry 1). In the presence of **I**, cyclooctene was smoothly oxidized at 305 K to give 1,2-epoxycyclooctane in 97 % yield based on H_2O_2 (Table 1, entry 2). When lowering the reaction temperature to 273 K, the epoxidation still significantly proceeded (Table 1, entry 3). Even under the stoichiometric conditions using one equivalent of H_2O_2 with respect to cyclooctene, 1,2-epoxycyclooctane was obtained in 94 % yield (Table 1, entry 4). The amount of **I** could be much reduced; even when using 0.1 mol% of **I** (with respect to H_2O_2), 1,2-epoxycyclooctane was produced in 94 % yield (Table 1, entry 5). The catalytic activities of the precursors of **I** were much lower than that of **I**; the epoxidation using PW10 and $\text{TiO}(\text{acac})_2$ afforded 1,2-epoxycyclooctane in only 12 % and 4 % yields, respectively (Table 1, entries 6 and 7). As above-mentioned, **I** could readily be formed by just mixing PW10 and $\text{TiO}(\text{acac})_2$ in CH_3CN . Thus, it should be noted that a simple mixture of PW10 and $\text{TiO}(\text{acac})_2$ (so-called “in-situ-prepared catalyst”) could be utilized for the epoxidation and that the in-situ-prepared catalyst showed almost the same performance as that of **I** (Table 1, entry 8). It would be very advantageous to demonstrate the reactions using such in-situ-prepared catalysts because there is no need to synthesize (isolate) the catalysts separately. Hence, several efficient POM-based in-situ-prepared catalyst systems in aqueous media²⁵ as well as

Submitted to *Catal. Sci. Technol.* as an Article (revised)

in organic media¹⁹ have been developed to date.

Up to the present, several Ti-substituted POMs for H₂O₂-based oxidation have been reported.⁴ The catalytic performance of **I** was much superior to those of the previously reported Ti-substituted POMs including our silicotungstate analogue TBA₈[(γ -SiW₁₀O₃₆)₂Ti₄(μ -O)₂(μ -OH)₄] (Table S3).⁴ As we expected, the effect of the central heteroatoms was very significant; the reaction rate of **I** under the conditions described in Fig. S4 was 2.7 mM min⁻¹ and ca. 11 times larger than that of TBA₈[(γ -SiW₁₀O₃₆)₂Ti₄(μ -O)₂(μ -OH)₄] (0.26 mM min⁻¹). By changing the central heteroatom from Si⁴⁺ to P⁵⁺, the negative charge of the POM anion decreases, and thereby the catalytic activity for electrophilic oxidation is likely improved. This is one possible explanation of the effect of the central heteroatoms, and such effect is also observed in the case of V-substituted POMs.²⁰

During the catalytic oxidation, no degradation of **I** into smaller molecular weight peroxotungstate species, such as [HPO₄{WO(O₂)₂}₂]²⁻ and [PO₄{WO(O₂)₂}₄]³⁻, was observed. When adding an excess amount of diethyl ether to the reaction solution, **I** dissolved in the solution could spontaneously precipitate out, and thus the used **I** after the reaction could easily be recovered by simple filtration (precipitation method, $\geq 90\%$ recovery). Moreover, the recovered **I** could be reused at least five times with keeping its high catalytic performance for the same reaction (Fig. 5). It should be noted that the IR, CSI-MS, and ³¹P NMR spectra of the recovered **I** catalyst even after the fifth reuse experiment were almost the same as those of the as-prepared fresh **I**, showing the high durability of **I** (Fig. S1d, S2c, and S5).

Next, the synthetic scope of the present **I**-catalyzed oxidation system was investigated. In the presence of catalytic amounts of **I**, epoxidation of alkenes, oxygenation of sulfides, oxidative bromination of unsaturated compounds, and the hydroxylation of anisole with H₂O₂ efficiently proceeded to give the corresponding oxidation products. As for epoxidation, various kinds of structurally diverse alkenes including cyclic, internal, and terminal ones could be converted into the corresponding epoxides with high selectivities (Table 2). In contrast with porous titanasilicate-based catalysts, the epoxidation of relatively bulky alkenes, e.g., norbornene, cyclooctene and

Submitted to *Catal. Sci. Technol.* as an Article (revised)

cyclododecene, efficiently proceeded (Table 2, entries 1–3). A non-activated terminal alkene of 1-octene could also be converted into the corresponding epoxide (Table 2, entry 8). For the epoxidation of *cis*- and *trans*-alkenes, the configurations around the C=C were completely retained in the corresponding epoxides (Table 2, entries 5–7), indicating no involvement of free-radical intermediates in the present **I**-catalyzed epoxidation. In the epoxidation of *cis*- and *trans*-2-octenes, the yield of *cis*-2,3-epoxyoctane was significantly higher than that of *trans*-2,3-epoxyoctane, while the $\pi(\text{C}=\text{C})$ HOMO energy of *cis*-2-octene (–0.342 eV) calculated at the HF/6-311G(d,p) level was almost the same as that of *trans*-2-octene (–0.343 eV) (Table 2, entries 5 and 6). Moreover, the epoxidation of 3-methyl-1-cyclohexene was highly diastereoselective and afforded the corresponding epoxide with the epoxy ring *trans* to the methyl group (*anti* configuration) (Table 2, entry 4). Such stereospecific *cis*-preferential and diastereoselective *anti*-preferential epoxidations are not common and likely owing to the steric effect of the active oxygen species generated on POMs.²⁰

The present **I**-catalyzed oxidation system was also applicable to oxygenation of sulfides (Table 3). The reaction completed within 10 min and afforded the corresponding oxygenated products in $\geq 90\%$ total yields based on H_2O_2 . The oxygenation of thioanisole and its derivatives with electron-donating as well as electron-withdrawing substituents on the phenyl rings efficiently proceeded (Table 3, entries 1–5). With regard to 4-cyanothioanisole, the reaction exclusively took place at the sulfide group, and no Payne-type reaction occurred at the cyano group (Table 3, entry 5). Not only aryl sulfides but also less reactive alkyl ones could effectively be oxygenated (Table 3, entries 6 and 7). Furthermore, **I** could efficiently catalyze oxidative bromination of various types of unsaturated compounds such as arenes, alkenes, and alkynes to give the corresponding mono- or dibrominated compounds in high yields, and the selected examples are summarized in Scheme 1. The hydroxylation of anisole could also be accomplished by using the present system and preferentially took place the *para*-position (Scheme 2). As can be seen from the above-mentioned results, one may recognize the broad synthetic utility of the present **I**-catalyzed oxidation system.

Submitted to *Catal. Sci. Technol.* as an Article (revised)

Identification of active oxygen species

With regard to our previously reported H₂O₂-based oxidation catalyzed by TBA₈[(γ -SiW₁₀O₃₆)₂Ti₄(μ -O)₂(μ -OH)₄]^{4a} and TBA_{*n*}[γ -XW₁₀O₃₈V₂(μ -OH)₂] (X = Si (*n* = 4) or P (*n* = 3)),²⁰ the Ti₂(μ -OOH)(μ -OH) and V₂(μ - η^2 : η^2 -O₂) species have been postulated as the respective active oxygen species on the basis of the spectroscopic, kinetic, and/or computational evidences. However, the isolation of the V₂(μ - η^2 : η^2 -O₂) species and even the detection of the Ti₂(μ -OOH)(μ -OH) species have not yet been successful because their concentrations are very low and/or they are not stable enough for isolation and/or detection.

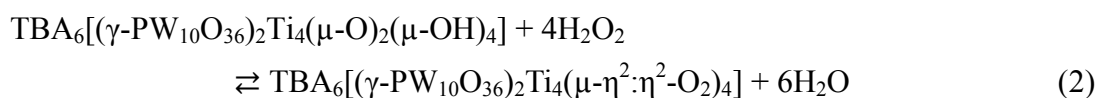
We initially measured the NMR (³¹P and ¹⁸³W) and CSI-MS spectra of the in-situ-formed active oxygen species by the reaction of **I** with H₂O₂. As above-mentioned, the ³¹P NMR spectrum of **I** showed a single signal at -11.8 ppm (Fig. 6a). Upon addition of an excess amount of H₂O₂ (128 equivalents with respect to **I**) to the CD₃CN solution of **I**, the ³¹P NMR signal due to **I** completely disappeared, and one new signal appeared at -16.7 ppm (Fig. 6b). Upon addition of cyclooctene (128 equivalents with respect to **I**) to this solution, the signal at -16.7 ppm completely disappeared, and the signal at -11.8 ppm due to **I** appeared again with the concomitant formation of 1,2-epoxycyclooctane (Fig. 6c). Therefore, the -16.7-ppm signal would be due to the active oxygen species (**II**) for the epoxidation. The ¹⁸³W NMR spectrum of **I** with H₂O₂ (64 equivalents with respect to **I**) in a mixed solvent of CD₃CN and PC (1:1 v/v) showed six signals at -94.3, -110.2, -112.9, -118.7, -123.2, and -127.2 ppm with the respective intensity ratio of 2:1:2:1:2:2 (Fig. 6f).²⁴ The ¹⁸³W NMR result indicates that **II** would possess the C_{2v} or C_{2h} symmetry.

The ³¹P NMR spectrum of the in-situ-formed **II** was almost unchanged and no signals of low molecular weight peroxotungstate fragments, such as [HPO₄{WO(O₂)₂}₂]²⁻ and [PO₄{WO(O₂)₂}₄]³⁻ (typically observed at 2.8 and 4.5 ppm in CD₃CN, respectively^{8c}), were observed even after the solution was kept for 24 h at room temperature. These results clearly indicate that **II** is highly stable and that the decomposition of [γ -PW₁₀O₃₆]⁷⁻ framework in **I** does not occur at all even in the presence of excess amounts of H₂O₂. Due to the stability as well as the relatively higher concentration of **II**, we

Submitted to *Catal. Sci. Technol.* as an Article (revised)

assumed that **II** can be isolated as the single species.

As we expected, **II** could readily be isolated by addition of an excess amount of diethyl ether to the CH₃CN solution containing **I** and H₂O₂ at 273 K. Furthermore, the single crystals of **II** for X-ray crystallographic analysis were successfully obtained by recrystallization of the isolated **II** from a mixed solvent of nitroethane (EtNO₂) and EtOAc at 278 K. The ³¹P NMR in CD₃CN spectrum of the single crystals was the same as that of the in-situ-formed **II** (Fig. 6d). The CSI-MS spectrum in CH₃CN showed the main set of signals centered at *m/z* = 3705 assignable to [TBA₈{(PW₁₀O₃₆)₂Ti₄(O₂)₄}·TBAOH]²⁺ (Fig. S2d). Because the single crystals of **II** were quite easily damaged by X-ray irradiation, the diffraction data were carefully collected by continuously changing the irradiation spots at the synchrotron facility (see the Experimental Section in detail). Consequently, we could manage to determine the anion structure of **II** with four peroxo species. Although highly disordered TBA cations could not crystallographically be assigned, the elemental analysis revealed the presence of six TBA cations per **II** anion. The anion structure of **II** is shown in Fig. 7, and the crystallographic data are summarized in Table S1. Two Ti atoms in the lacunary pocket of each [γ-PW₁₀O₃₆]⁷⁻ subunit were linked by one μ-η²:η²-O₂ species, and two monomer subunits were linked by two μ-η²:η²-O₂ species, that is, the presence of four Ti₂-μ-η²:η²-peroxo species in **II**. The anion structure of **II** was C_{2v} symmetry in agreement with the ¹⁸³W NMR spectrum of the in-situ-formed **II** (Fig. 6f). The elemental analysis data showed TBA/P/W/Ti ratio of 3:1:10:2. The stoichiometric oxidation of triphenylphosphine with **II** (10 μmol) gave ca. four equivalents (42 μmol) of triphenylphosphine oxide based on **II**, showing the presence of four active oxygen species in **II**. These data indicate that the formula of **II** is TBA₆[(γ-PW₁₀O₃₆)₂Ti₄(μ-η²:η²-O₂)₄], and **II** can be formed by the reaction of **I** with four equivalents of H₂O₂ [eqn (2)].



Submitted to *Catal. Sci. Technol.* as an Article (revised)

With regard to the μ -oxo- μ - η^2 : η^2 -peroxo Ti(salan) complex reported by Katsuki and co-workers,^{3c} one μ - η^2 : η^2 -O₂ species, and two N atoms and two O atoms in the salan ligand were coordinated to each Ti atom in a pseudooctahedral arrangement (Fig. 1b), resulting in the coordination number of each Ti atom of seven. On the other hand, two O atoms in POM framework and two μ - η^2 : η^2 -O₂ species were coordinated to each Ti atom in a pseudotetrahedral arrangement and there was no bridging μ -O ligand between Ti atoms in the case of **II**. Thus, the coordination number of each Ti atom in **II** was six. This is the most significant difference between **II** and the inactive Katsuki's complex, and thus we assume that the high catalytic performance of **I** would be ascribed to the formation of the active pseudotetrahedral Ti peroxo species, in good agreement with the high reactivity of tetrahedral titanium species (within zeolite framework).^{2,12}

Besides the above phosphine oxidation, the stoichiometric epoxidation of cyclooctene and thioanisole with **II** (4 μ mol) also gave ca. four equivalents of 1,2-epoxycyclooctane (17 μ mol) and the corresponding oxygenated products (methyl phenyl sulfoxide: 7 μ mol, methyl phenyl sulfone: 5 μ mol), respectively, with respect to **II**, showing that all of the four Ti₂- μ - η^2 : η^2 -peroxo species in **II** are active for these oxidations. Although to date several compounds with M₂- μ - η^2 : η^2 -peroxo species (M = Ti,^{3c} Zr,^{26a-c} Hf,^{26a-c} U,^{26d,e} etc.) have been synthesized and their structures have been determined, these peroxo species are not active for epoxidation. To the best of our knowledge, **II** is the first example of the structurally determined M₂- μ - η^2 : η^2 -peroxo species which are truly active for epoxidation. The reaction rate (0.043 mM min⁻¹) of the “stoichiometric” epoxidation of cyclooctene (0.035 M) with **II** (0.57 mM) agreed well with that (0.041 mM min⁻¹) of the “catalytic” epoxidation of cyclooctene (0.035 M) with H₂O₂ (0.14 M) by **I** (0.57 mM) (Fig. S6), indicating that **II** is the truly active oxygen species and included in the catalytic cycle for the present **I**-catalyzed oxidation.

Conclusion

In this work, we have obtained several important findings for the POM-based catalyst design and the application to H₂O₂-based oxidation. Firstly, we could synthesize an organic solvent-soluble divacant

Submitted to *Catal. Sci. Technol.* as an Article (revised)

lacunary phosphotungstate PW10 for the first time. By the reaction of PW10 and $\text{TiO}(\text{acac})_2$ in CH_3CN , a novel Ti-substituted phosphotungstate **I** could readily be synthesized. The synthetic strategy using an organic solvent-soluble lacunary precursor in an organic medium demonstrated herein will be applicable to synthesis of various types of metal-substituted POMs and open up a new avenue for POM chemistry and synthesis. In the presence of **I**, several H_2O_2 -based oxidation reactions, such as epoxidation of alkenes, oxygenation of sulfides, oxidative bromination of unsaturated compounds, and the hydroxylation of anisole, smoothly proceeded to afford the corresponding oxidation products with high efficiencies and selectivities, and the catalytic performance of **I** was much superior to those of the previously reported Ti-substituted POMs including our silicotungstate analogue $\text{TBA}_8[(\gamma\text{-SiW}_{10}\text{O}_{36})_2\text{Ti}_4(\mu\text{-O})_2(\mu\text{-OH})_4]$. Moreover, **I** was highly durable during the catalysis (no degradation into smaller molecular weight peroxotungstate species) and could be reused several times with keeping its high catalytic performance. The in-situ-prepared catalyst by just mixing PW10 and $\text{TiO}(\text{acac})_2$ was also equally effective to **I**, which would be advantageous for practical applications. Fortunately, we could isolate the truly catalytically active species for the present **I**-catalyzed H_2O_2 -based oxidation (**II**), and its structure could successfully be determined by X-ray crystallographic analysis. Compound **II** possessed four $\text{Ti}_2\text{-}\mu\text{-}\eta^2\text{:}\eta^2\text{-peroxo}$ species, and all of the four peroxo species were active for oxidation. To the best of our knowledge, **II** is the first example of structurally determined $\text{M}_2\text{-}\mu\text{-}\eta^2\text{:}\eta^2\text{-peroxo}$ species truly active for oxidation, which is included in the catalytic cycle for the present **I**-catalyzed oxidation. We hope that these findings will lead to new insight into chemistry of active oxygen species.

Experimental section

Materials

TBABr, $\text{TiO}(\text{acac})_2$, and EtNO_2 were obtained from TCI, and used as received. HNO_3 , diethyl ether, CH_3CN , EtOAc, 30 % H_2O_2 , acetone, PC, methanol, and deuterated solvents (CD_3CN and

Submitted to *Catal. Sci. Technol.* as an Article (revised)

DMSO-*d*₆) were obtained from KANTO Chemical, and used as received. Substrates were obtained from Sigma-Aldrich, TCI, KANTO Chemical, and Wako Pure Chemical Industries, and purified prior to the use (if necessary).²⁷ Cs₇[γ -PW₁₀O₃₆]²² and TBA₈[(γ -SiW₁₀O₃₆)₂Ti₄(μ -O)₂(μ -OH)₄]^{4a} were synthesized according to the reported procedures. Aqueous 90% H₂O₂ was prepared by concentration of 30 % H₂O₂.

Instruments

IR spectra were measured on Jasco FT/IR-4100 using KBr or KCl disks. NMR spectra were measured at room temperature on JEOL JNM-EX270 (³¹P, 109 MHz) or JEOL JNM-ECA500 (¹H, 500 MHz; ³¹P, 202 MHz; ¹⁸³W, 20.6 MHz). Chemical shifts (δ) of ¹H, ³¹P and ¹⁸³W were reported in ppm downfield from internal TMS, external 85 % H₃PO₄ (in D₂O), and external 1 M Na₂WO₄ (in D₂O), respectively. NMR measurements were done in different solvents. The solvent selection is simply the solubility reason. Cold-spray ionization mass (CSI-MS) spectra were recorded on JEOL JMS-T100CS. Typical measurements were as follows: Orifice voltage 135 V for positive ions; concentration 0.1 mM; spray temperature 263 K; ion source at room temperature. ICP-AES analyses were performed on Shimadzu ICPS-8100. Elemental analyses for C, H, and N were performed on Yanaco MT-6. GC analyses were performed on Shimadzu GC-2014 with a flame ionization detector (FID) equipped with a Stabilwax capillary column (internal diameter = 0.25 mm, length = 30 m). GC-MS spectra were measured on Shimadzu GCMS-QP2010 at an ionization voltage 70 eV. HPLC analyses were performed on Shimadzu Prominence system with a UV-vis detector (Shimadzu SPD-20A, 270 nm) equipped with a GL Science Inertsil ODS-3 column (particle size = 5 μ m, internal diameter = 4.6 mm ϕ , length = 250 mm), using a mixed solvent of methanol and water as the eluent (9:1 v/v). The π (C=C) HOMO energies of *cis*- and *trans*-2-octenes were calculated at the HF/6-311G(d,p) level with the Gaussian 09 program package.²⁸

X-ray crystallography

Diffraction measurements of **I** were made on Rigaku MicroMax-007 Saturn 724 CCD detector with

Submitted to *Catal. Sci. Technol.* as an Article (revised)

graphite monochromated Mo K α radiation ($\lambda = 0.71069 \text{ \AA}$) at 123 K. The diffraction data of **I** were collected using CrystalClear.²⁹ Diffraction measurements of **II** were made on BL1A beamline in KEK Photon Factory (synchrotron facility) with a diffractometer equipped with Dectris Pilatus 2M-F PAD detector ($\lambda = 0.95000 \text{ \AA}$) at 95 K. The diffraction data of **II** were collected using ugui program. All the data were processed using HKL2000.³⁰ Neutral scattering factors were obtained from the standard source. In the reduction of data, Lorentz and polarization corrections were made. All structures were solved by SHELXS-97 (direct methods) and refined by SHELXH-97.³¹ The structural analysis was performed using CrystalStructure,³² Win-GX,³³ and Yadokari-XG.³⁴ The metal atoms (P, W, and Ti) in **I** were refined anisotropically. The metal atoms (P, W, and Ti) and oxygen atoms in **II** were refined anisotropically with SIMU. Some of the bond lengths of **II** were refined with SADI and DFIX. The highly disordered TBA cations of **II** could not crystallographically be assigned and were omitted by using SQUEEZE program of PLATON,³⁵ affording much improved analytical results. CCDC-1406336 (**I**) and CCDC-1406337 (**II**) contain the supplementary crystallographic data for this manuscript. The data can be obtained free of charge via www.ccdc.cam.ac.uk/conts/retrieving.html (or from the Cambridge Crystallographic Data Centre, 12, Union Road, Cambridge CB2 1EZ, UK; Fax: (+44) 1223-336-033; or deposit@ccdc.cam.ac.uk).

BVS calculations

The BVS values were calculated by the expression for the variation of the length r_{ij} of a bond between two atoms i and j in observed crystal with valence V_i :

$$V_i = \sum_j \exp\left(\frac{r'_0 - r_{ij}}{B}\right)$$

where B is constant equal to 0.37 \AA , r'_0 is bond valence parameter for a given atom pair.³⁶

Catalytic oxidation

The catalytic oxidations were carried out in a 15 mL glass tube reactor containing a magnetic stir bar. A typical procedure was as follows: **I**, substrate, 30% H₂O₂, and CH₃CN were successively placed into the glass tube reactor. The reaction mixture was stirred at 305 K. The yields of products were

Submitted to *Catal. Sci. Technol.* as an Article (revised)

determined by GC analysis using an internal standard. All products are known and confirmed by comparison of their GC retention times and/or GC-MS patterns with the authentic samples.

Stoichiometric oxidation

The stoichiometric oxidations were carried out in a 15 mL glass tube reactor containing a magnetic stir bar. A typical procedure for the stoichiometric epoxidation of cyclooctene was as follows: Cyclooctene (0.25 mmol) and CH₃CN (6.96 mL) were successively placed into a glass tube reactor. After the solution was stirred at 253 K, the reaction was initiated by addition of **II** (4 μmol). The reaction was periodically monitored by GC. Reaction rates (R_0) were determined from the slopes of reaction profiles ([epoxide] versus time) at low conversions of cyclooctene (initial rate method). Finally, ca. four equivalents of 1,2-epoxycyclooctane (17 μmol) were produced. The stoichiometric oxidation of thioanisole was carried out via the same procedure at room temperature, and gave ca. four equivalents of oxygenated products (methyl phenyl sulfoxide: 7 μmol, methyl phenyl sulfone: 5 μmol). A typical procedure for the stoichiometric oxidation of triphenylphosphine was as follows: triphenylphosphine (0.25 mmol) and CH₃CN (4 mL) were successively placed into a glass tube reactor. After the solution was stirred at 305 K, the reaction was initiated by addition of **II** (10 μmol). The reaction was periodically monitored by HPLC. Finally, ca. four equivalents (42 μmol) of triphenylphosphine oxide were produced.

Synthesis of PW10

TBABr (0.67 g, 2.1 mmol) was dissolved in HNO₃ (2.6 M, 200 mL) at 273 K. Then, Cs₇[γ-PW₁₀O₃₆]·H₂O (2.0 g, 0.59 mmol) was added in a single step, and the resulting solution was stirred for 10 min. The resulting white precipitate of PW10 was collected by filtration, washed with water (100 mL) and diethyl ether (200 mL) to afford analytically pure white powder of PW10 (1.6 g, 84% yield based on Cs₇[γ-PW₁₀O₃₆], >99% purity). Compound PW10 was stored in a freezer (at 253 K). To prevent the isomerization and/or decomposition of PW10, the vacuum drying and the storage at room temperature should be avoided. Elemental analysis calcd (%) for C₄₈H₁₁₈N₃O₃₉PW₁₀

Submitted to *Catal. Sci. Technol.* as an Article (revised)

(TBA₃[PW₁₀O₃₄(H₂O)₂] \cdot 3H₂O): C, 17.84; H, 3.68; N, 1.30; P, 0.96; W, 56.90. Found: C, 17.65; H, 3.53; N, 1.21; P, 0.92; W, 56.50. IR (KBr pellet; 4000–400 cm⁻¹): 3429, 2962, 2935, 2874, 1625, 1483, 1381, 1347, 1151, 1109, 1057, 1036, 975, 951, 861, 798, 675, 661, 613, 535, 401 cm⁻¹. ³¹P NMR (DMSO-*d*₆): δ -10.5 ppm. ¹⁸³W NMR (DMSO-*d*₆): δ -105.4, -114.2, -117.3, -136.1, -168.5 ppm (the integrated intensity ratio of 1:1:1:1). CSI-MS (acetone): *m/z* = 3384 [TBA₄(PW₁₀O₃₄)]⁺.

Synthesis of compound I

TiO(acac)₂ (0.16 g, 0.62 mmol) was dissolved in CH₃CN (20 mL) at room temperature. Then, PW10 (1.0 g, 0.31 mmol) was added in a single step, and the resulting solution was stirred for 5 min. After filtration, the solution was added to diethyl ether (200 mL) and the resulting pale yellow precipitate was collected by filtration. The crude compound was purified by recrystallization from a mixed solvent of CH₃CN and EtOAc. The solution was kept at room temperature for 24 h to afford pale yellow crystals of **I** (0.47 g, 45% yield based on PW10). Elemental analysis calcd (%) for C₁₀₀H₂₃₀N₆O₈₁P₂Ti₄W₂₀ (TBA₆[(PW₁₀O₃₆)₂Ti₄O₂(OH)₄] \cdot EtOAc \cdot H₂O): C, 17.81; H, 3.44; N, 1.25; P, 0.92; Ti, 2.84; W, 54.53. Found: C, 18.25; H, 3.51; N, 1.15; P, 0.98; Ti, 2.53; W, 55.60. IR (KBr pellet; 4000–400 cm⁻¹): 3580, 3446, 2962, 2934, 2874, 1732, 1623, 1483, 1379, 1246, 1152, 1070, 1050, 1040, 971, 956, 878, 815, 656, 537, 489, 420 cm⁻¹. ¹H NMR (CD₃CN): δ 7.91 (μ -OH, 4H), 4.06 (EtOAc, 2H), 3.17 (TBA, 48H), 1.97 (EtOAc, 3H), 1.67 (TBA, 48H), 1.43 (TBA, 48H), 1.20 (EtOAc, 3H), 1.01 (TBA, 72H) ppm. ³¹P NMR (CD₃CN): δ -11.8 ppm. ¹⁸³W NMR (CD₃CN/PC (1:1 v/v)): δ -110.6, -112.7, -115.8 ppm (the integrated intensity ratio of 1:2:2). CSI-MS (CH₃CN): *m/z* = 3561 [TBA₈H₄{(PW₁₀O₃₆)₂Ti₄O₆}]²⁺, 3674 [TBA₉H{(PW₁₀O₃₆)₂Ti₄O₅}]²⁺, 6880 [TBA₇H₄{(PW₁₀O₃₆)₂Ti₄O₆}]⁺.

Synthesis of compound II

Compound **I** (0.10 g, 0.015 mmol) was dissolved in CH₃CN (5 mL) at 273 K. Then, 90% H₂O₂ (128 equivalents, 1.9 mmol) was added in a single step, and the resulting solution was stirred for 1 h.

Submitted to *Catal. Sci. Technol.* as an Article (revised)

After filtration, the solution was added to diethyl ether (50 mL) and the resulting yellow precipitate was collected by filtration, and washed with EtOAc (20 mL). The pure compound **II** was obtained as yellow powder after dryness (0.072 g, 72% yield based on **I**). Elemental analysis calcd (%) for $C_{100}H_{228}N_6O_{84}P_2Ti_4W_{20}$ ($TBA_6[(PW_{10}O_{36})_2Ti_4(O_2)_4] \cdot EtOAc \cdot 2H_2O$): C, 17.69; H, 3.38; N, 1.24; P, 0.91; Ti, 2.82; W, 54.16. Found: C, 17.10; H, 3.39; N, 1.20; P, 0.89; Ti, 2.81; W, 54.41. IR (KCl pellet; 4000–400 cm^{-1}): 3410, 2960, 2932, 2872, 1624, 1482, 1466, 1379, 1131, 1062, 1041, 972, 955, 879, 816, 759, 524, 460, 422 cm^{-1} . ^{31}P NMR (CD_3CN): δ –16.8 ppm. The pale yellow crystals of **II** suitable for the X-ray crystallographic analysis were obtained by recrystallization from a mixed solvent of $EtNO_2$ and EtOAc at 278 K. Elemental analysis calcd (%) for $C_{102}H_{233}N_7O_{86}P_2Ti_4W_{20}$ ($TBA_6[(PW_{10}O_{36})_2Ti_4(O_2)_4] \cdot EtNO_2 \cdot EtOAc \cdot 2H_2O$): C, 17.85; H, 3.42; N, 1.43; P, 0.90; Ti, 2.79; W, 53.57. Found: C, 17.96; H, 3.44; N, 1.42; P, 0.90; Ti, 2.66; W, 53.36. IR (KCl pellet; 4000–400 cm^{-1}): 3421, 2961, 2933, 2873, 1732, 1624, 1546, 1483, 1379, 1131, 1062, 1040, 971, 955, 880, 818, 759, 524, 459, 424 cm^{-1} . ^{31}P NMR (CD_3CN): δ –16.9 ppm. ^{183}W NMR (*in situ*, CD_3CN/PC (1:1 v/v)): δ –94.3, –110.2, –112.9, –118.7, –123.2, –127.2 ppm (the integrated intensity ratio of 2:1:2:1:2:2). CSI-MS (CH_3CN): m/z = 3705 (main set of signals) $[TBA_8\{(PW_{10}O_{36})_2Ti_4(O_2)_4\} \cdot TBAOH]^{2+}$.

Acknowledgements

We thank KEK Photon Factory (Research 2013G640) for the use of the X-ray diffraction instruments (BL1A beamline). This work was supported in part by the Japan Society for the Promotion of Science (JSPS) through its “Funding Program for World-Leading Innovative R&D on Science and Technology (FIRST Program)” and Grants-in-Aid for JSPS Fellows and Scientific Research from the Ministry of Education, Culture, Science, Sports, and Technology of Japan.

References and notes

- 1 R. A. Sheldon, I. Arends and U. Hanefeld, *Green Chemistry and Catalysis*, Wiley-VCH,

Submitted to *Catal. Sci. Technol.* as an Article (revised)

Weinheim, 2007.

- 2 Ti (zeolites): (a) M. Taramasso, G. Perego and B. Notari, U.S. Patent 4,410,501, 1983; (b) M. G. Clerici, *Appl. Catal.*, 1991, **68**, 249–261; (c) B. Notari, *Catal. Today*, 1993, **18**, 163–172; (d) T. Tatsumi, *Metal-Substituted Zeolites as Heterogeneous Oxidation Catalysts, Modern Heterogeneous Oxidation Catalysis* (Ed.: N. Mizuno), Wiley-VCH, Weinheim, 2009, pp. 125–155; (e) M. A. Camblor, A. Corma, A. Martínez and J. Pérez-Pariente, *J. Chem. Soc., Chem. Commun.*, 1992, 589–590; (f) P. Wu and Y. Tatsumi, *Chem. Commun.*, 2001, 897–898; (g) P. Wu, Y. Kubota and T. Yokoi, *ACS Catal.*, 2014, **4**, 23–30.
- 3 Ti (salen and salan complexes): (a) K. Matsumoto, Y. Sawada, B. Saito, K. Sakai and T. Katsuki, *Angew. Chem., Int. Ed.*, 2005, **44**, 4935–4939; (b) Y. Sawada, K. Matsumoto, S. Kondo, H. Watanabe, T. Ozawa, K. Suzuki, B. Saito and T. Katsuki, *Angew. Chem., Int. Ed.*, 2006, **45**, 3478–3480; (c) S. Kondo, K. Saruhashi, K. Seki, K. Matsubara, K. Miyaji, T. Kubo, K. Matsumoto and T. Katsuki, *Angew. Chem., Int. Ed.*, 2008, **47**, 10195–10198.
- 4 Ti (POMs): (a) Y. Goto, K. Kamata, K. Yamaguchi, K. Uehara, S. Hikichi and N. Mizuno, *Inorg. Chem.*, 2006, **45**, 2347–2356; (b) T. Yamase, E. Ishikawa, Y. Asai and S. Kanai, *J. Mol. Catal. A: Chem.*, 1996, **114**, 237–245; (c) L. Hua, Y. Qiao, Y. Yu, W. Zhu, T. Cao, Y. Shi, H. Li, B. Feng and Z. Hou, *New J. Chem.*, 2011, **35**, 1836–1841; (d) P. Jiménez-Lozano, I. D. Ivanchikova, O. A. Kholdeeva, J. M. Poblet and J. J. Carbó, *Chem. Commun.*, 2012, **48**, 9266–9268; (e) C. N. Kato, K. Hayashi, S. Negishi and K. Nomiya, *J. Mol. Catal. A: Chem.*, 2007, **262**, 25–29; (f) E. Ishikawa and T. Yamase, *J. Mol. Catal. A: Chem.*, 1999, **142**, 61–76; (g) B. G. Donoeva, T. A. Trubitsina, N. S. Antonova, J. J. Carbó, J. M. Poblet, G. Al-Kadamany, U. Kortz and O. A. Kholdeeva, *Eur. J. Inorg. Chem.*, 2010, 5312–5317; (h) O. A. Kholdeeva, *Eur. J. Inorg. Chem.*, 2013, 1595–1605.
- 5 V: (a) A. Butler, M. J. Clague and G. E. Meister, *Chem. Rev.*, 1994, **94**, 625–638; (b) V. Conte and B. Floris, *Dalton Trans.*, 2011, **40**, 1419–1436; (c) D. Wischang, O. Brücher and J. Hartung, *Coord. Chem. Rev.*, 2011, **255**, 2204–2217.

Submitted to *Catal. Sci. Technol.* as an Article (revised)

- 6 Mn: (a) P. Battioni, J. P. Renaud, J. F. Bartoli, M. Reina-Artiles, M. Fort and D. Mansuy, *J. Am. Chem. Soc.*, 1988, **110**, 8462–8470; (b) D. E. De Vos, B. F. Sels, M. Reynaers, Y. V. S. Rao and P. A. Jacobs, *Tetrahedron Lett.*, 1998, **39**, 3221–3224; (c) B. S. Lane, M. Vogt, V. J. DeRose and K. Burgess, *J. Am. Chem. Soc.*, 2002, **124**, 11946–11954; (d) P. Saisaha, J. W. de Boer and W. R. Browne, *Chem. Soc. Rev.*, 2013, **42**, 2059–2074.
- 7 Fe: (a) M. Costas, K. Chen and L. Que, Jr., *Coord. Chem. Rev.*, 2000, **200–202**, 517–544; (b) M. C. White, A. G. Doyle and E. N. Jacobsen, *J. Am. Chem. Soc.*, 2001, **123**, 7194–7195; (c) M. S. Chen and M. C. White, *Science*, 2007, **318**, 783–787; (d) E. P. Talsi, K. P. Bryliakov and *Coord. Chem. Rev.*, 2012, **256**, 1418–1434.
- 8 W: (a) K. Kamata, K. Yonehara, Y. Sumida, K. Yamaguchi, S. Hikichi and N. Mizuno, *Science*, 2003, **300**, 964–966; (b) R. Noyori, M. Aoki and K. Sato, *Chem. Commun.*, 2003, 1977–1986; (c) K. Kamata, T. Hirano, S. Kuzuya and N. Mizuno, *J. Am. Chem. Soc.*, 2009, **131**, 6997–7004; (d) R. Ishimoto, K. Kamata and N. Mizuno, *Angew. Chem., Int. Ed.*, 2012, **51**, 4662–4665; (e) C. Venturello, E. Alneri and M. Ricci, *J. Org. Chem.*, 1983, **48**, 3831–3833; (f) Y. Ishii, K. Yamawaki, T. Yoshida, T. Ura and M. Ogawa, *J. Org. Chem.*, 1987, **52**, 1868–1870; (g) K. Sato, M. Aoki, M. Ogawa, T. Hashimoto and R. Noyori, *J. Org. Chem.*, 1996, **61**, 8310–8311; (h) K. Sato, M. Aoki and R. Noyori, *Science*, 1998, **281**, 1646–1647.
- 9 Re: (a) J. Rudolph, K. L. Reddy, J. P. Chiang and K. B. Sharpless, *J. Am. Chem. Soc.*, 1997, **119**, 6189–6190; (b) W. A. Herrmann, R. M. Kratzer, H. Ding, W. R. Thiel and H. Glas, *J. Organomet. Chem.*, 1998, **555**, 293–295; (c) H. Adolfsson, C. Copéret, J. P. Chiang and A. K. Yudin, *J. Org. Chem.*, 2000, **65**, 8651–8658; (d) P. Altmann, M. Cokoja and F. E. Kühn, *Eur. J. Inorg. Chem.* 2012, 3235–3239.
- 10 Pt: (a) M. Colladon, A. Scarso, P. Sgarbossa, R. A. Michelin and G. Strukul, *J. Am. Chem. Soc.*, 2006, **128**, 14006–14007; (b) M. Colladon, A. Scarso, P. Sgarbossa, R. A. Michelin and G. Strukul, *J. Am. Chem. Soc.*, 2007, **129**, 7680–7689; (c) A. N. Vedernikov, *Acc. Chem. Res.*, 2012, **45**, 803–813.

Submitted to *Catal. Sci. Technol.* as an Article (revised)

- 11 (a) R. A. Sheldon and J. K. Kochi, *Metal Catalyzed Oxidations of Organic Compounds*, Academic Press, New York, 1981; (b) M. Hudlicky, *Oxidations in Organic Chemistry*, ACS Monograph Series, American Chemical Society, Washington, DC, 1990; (c) *Modern Oxidation Methods* (Ed.: J.-E. Bäckvall), Wiley-VCH: Weinheim, 2004.
- 12 (a) W. Y. Lin and H. Frei, *J. Am. Chem. Soc.*, 2002, **124**, 9292–9298; (b) S. Bordiga, A. Damin, F. Bonino, G. Ricchiardi, C. Lamberti and A. Zecchina, *Angew. Chem., Int. Ed.*, 2002, **41**, 4734–4737; (c) D. H. Wells, Jr., W. N. Delgass and K. T. Thomson, *J. Am. Chem. Soc.*, 2004, **126**, 2956–2962; (d) S. Bordiga, F. Bonino, A. Damin and C. Lamberti, *Phys. Chem. Chem. Phys.*, 2007, **9**, 4854–4878; (e) L. Wang, G. Xiong, J. Su, P. Li and H. Guo, *J. Phys. Chem. C*, 2012, **116**, 9122–9131.
- 13 N. Mizuno, K. Yamaguchi and K. Kamata, *Catal. Surv. Asia*, 2011, **15**, 68–79.
- 14 (a) C. L. Hill and M. Prosser-McCartha, *Coord. Chem. Rev.*, 1995, **143**, 407–455; (b) N. Mizuno, K. Yamaguchi and K. Kamata, *Coord. Chem. Rev.*, 2005, **249**, 1944–1956; (c) N. Mizuno, K. Kamata, S. Uchida and K. Yamaguchi, *Liquid-Phase Oxidations with Hydrogen Peroxide and Molecular Oxygen Catalyzed by Polyoxometalate-Based Compounds, Modern Heterogeneous Oxidation Catalysis* (Ed.: N. Mizuno), Wiley-VCH, Weinheim, 2009, pp. 185–216.
- 15 (a) K. Kamata, K. Yonehara, Y. Nakagawa, K. Uehara and N. Mizuno, *Nat. Chem.*, 2010, **2**, 478–483; (b) K. Kamata, T. Yamaura and N. Mizuno, *Angew. Chem., Int. Ed.*, 2012, **51**, 7275–7278.
- 16 Y. Sakai, Y. Kitakoga, K. Hayashi, K. Yoza and K. Nomiya, *Eur. J. Inorg. Chem.*, 2004, 4646–4652.
- 17 By the reaction of $K_8[\gamma\text{-SiW}_{10}\text{O}_{36}]$ with TiOSO_4 in acidic solution (pH = 1.3) at room temperature, a dimeric Ti-substituted γ -Keggin POM, $[\text{Ti}_4(\gamma\text{-SiW}_{10}\text{O}_{36})_2(\mu\text{-O})_2(\mu\text{-OH})_4]^{8-}$, can be synthesized.^{4a} On the other hand, even using the same starting materials, a tetrameric Ti-substituted POM composed of β -Keggin subunits, $[(\beta\text{-Ti}_2\text{SiW}_{10}\text{O}_{39})_4]^{24-}$, is obtained when

Submitted to *Catal. Sci. Technol.* as an Article (revised)

- performing the synthesis at pH = 2 and 353 K. See: F. Hussain, B. S. Bassil, L.-H. Bi, M. Reicke and U. Kortz, *Angew. Chem., Int. Ed.*, 2004, **43**, 3485–3488.
- 18 H. Liu, J. Peng, Z. Su, Y. Chen, B. Dong, A. Tian, Z. Han and E. Wang, *Eur. J. Inorg. Chem.*, 2006, 4827–4833.
- 19 (a) Y. Kikukawa, K. Yamaguchi and N. Mizuno, *Angew. Chem., Int. Ed.*, 2010, **49**, 6096–6100; (b) Y. Kikukawa, K. Suzuki, M. Sugawa, T. Hirano, K. Kamata, K. Yamaguchi and N. Mizuno, *Angew. Chem., Int. Ed.*, 2012, **51**, 3686–3690; (c) Y. Kikukawa, Y. Kuroda, K. Yamaguchi and N. Mizuno, *Angew. Chem., Int. Ed.*, 2012, **51**, 2434–2437; (d) T. Hirano, K. Uehara, K. Kamata and N. Mizuno, *J. Am. Chem. Soc.*, 2012, **134**, 6425–6433; (e) K. Suzuki, F. Tang, Y. Kikukawa, K. Yamaguchi and N. Mizuno, *Angew. Chem., Int. Ed.*, 2014, **53**, 5356–5360; (f) K. Suzuki, M. Sugawa, Y. Kikukawa, K. Kamata, K. Yamaguchi and N. Mizuno, *Inorg. Chem.*, 2012, **51**, 6953–6961.
- 20 K. Kamata, K. Sugahara, K. Yonehara, R. Ishimoto and N. Mizuno, *Chem. – Eur. J.*, 2011, **17**, 7549–7559.
- 21 (a) P. J. Domaille and R. L. Harlow, *J. Am. Chem. Soc.*, 1986, **108**, 2108–2109; (b) A. Patel and K. Patel, *Polyhedron*, 2014, **69**, 110–118; (c) E. Cadot, V. Béreau and F. Sécheresse, *Inorg. Chim. Acta*, 1996, **252**, 101–106; (d) C. Besson, Z. Huang, Y. V. Geletii, S. Lense, K. I. Hardcastle, D. G. Musaev, T. Lian, A. Proust and C. L. Hill, *Chem. Commun.*, 2010, **46**, 2784–2786.
- 22 P. J. Domaille, *Inorg. Synth.*, 1990, **27**, 96–104.
- 23 R. Tan, D. Li, H. Wu, C. Zhang and X. Wang, *Inorg. Chem. Commun.*, 2008, **11**, 835–836.
- 24 Because the solubility of **I** in CD₃CN was below the detection limit of ¹⁸³W nuclei, PC was added to dissolve **I** in the solvent. The ³¹P NMR spectrum of **I** after the ¹⁸³W NMR measurement showed a single signal at –11.8 ppm, suggesting that the structure of **I** was maintained during the ¹⁸³W NMR measurement.
- 25 (a) I. A. Weinstock, E. M. G. Barbuzzi, M. W. Wemple, J. J. Cowan, R. S. Reiner, D. M.

Submitted to *Catal. Sci. Technol.* as an Article (revised)

- Sonnen, R. A. Heintz, J. S. Bond and C. L. Hill, *Nature*, 2001, **414**, 191; (b) D. Sloboda-Rozner, P. L. Alster and R. Neumann, *J. Am. Chem. Soc.*, 2003, **125**, 5280.
- 26 (a) S. S. Mal, N. H. Nsouli, M. Carraro, A. Sartorel, G. Scorrano, H. Oelrich, L. Walder, M. Bonchio and U. Kortz, *Inorg. Chem.*, 2010, **49**, 7–9; (b) D. Li, H. Han, Y. Wang, X. Wang, Y. Li and E. Wang, *Eur. J. Inorg. Chem.*, 2013, 1926–1934; (c) B. S. Bassil, S. S. Mal, M. H. Dickman, U. Kortz, H. Oelrich and L. Walder, *J. Am. Chem. Soc.*, 2008, **130**, 6696–6697; (d) S. S. Mal, M. H. Dickman and U. Kortz, *Chem. – Eur. J.*, 2008, **14**, 9851–9855; (e) P. Miró, J. Ling, J. Qiu, P. C. Burns, L. Gagliardi and C. J. Cramer, *Inorg. Chem.*, 2012, **51**, 8784–8790.
- 27 *Purification of Laboratory Chemicals 5th ed.* (Eds.: D. D. Perrin, W. L. F. Armarego), Pergamon Press, Oxford, 2003.
- 28 Gaussian 09, Revision C.01, M. J. Frisch, G. W. Trucks, H. B. Schlegel, G. E. Scuseria, M. A. Robb, J. R. Cheeseman, G. Scalmani, V. Barone, B. Mennucci, G. A. Petersson, H. Nakatsuji, M. Caricato, X. Li, H. P. Hratchian, A. F. Izmaylov, J. Bloino, G. Zheng, J. L. Sonnenberg, M. Hada, M. Ehara, K. Toyota, R. Fukuda, J. Hasegawa, M. Ishida, T. Nakajima, Y. Honda, O. Kitao, H. Nakai, T. Vreven, J. A. Montgomery, Jr., J. E. Peralta, F. Ogliaro, M. Bearpark, J. J. Heyd, E. Brothers, K. N. Kudin, V. N. Staroverov, T. Keith, R. Kobayashi, J. Normand, K. Raghavachari, A. Rendell, J. C. Burant, S. S. Iyengar, J. Tomasi, M. Cossi, N. Rega, J. M. Millam, M. Klene, J. E. Knox, J. B. Cross, V. Bakken, C. Adamo, J. Jaramillo, R. Gomperts, R. E. Stratmann, O. Yazyev, A. J. Austin, R. Cammi, C. Pomelli, J. W. Ochterski, R. L. Martin, K. Morokuma, V. G. Zakrzewski, G. A. Voth, P. Salvador, J. J. Dannenberg, S. Dapprich, A. D. Daniels, O. Farkas, J. B. Foresman, J. V. Ortiz, J. Cioslowski and D. J. Fox, Gaussian, Inc., Wallingford CT, 2010.
- 29 (a) *CrystalClear 1.4.0*; Rigaku and Rigaku/MSO, The Woodlands, TX, 1999. b) J. W. Pflugrath, *Acta Crystallogr.*, 1999, **D55**, 1718–1725.
- 30 Z. Otwinowski and W. Minor, *Processing of X-ray Diffraction Data Collected in Oscillation Mode, Methods in Enzymology* (Eds.: C. W. Carter, Jr., R. M. Sweet), Macromolecular

Submitted to *Catal. Sci. Technol.* as an Article (revised)

Crystallography, Part A, Academic Press, New York, 1997, Vol. 276, pp. 307–326.

- 31 G. M. Sheldrick, *SHELX97, Programs for Crystal Structure Analysis*, Release 97-2, University of Göttingen: Göttingen, Germany, 1997.
- 32 *CrystalStructure 4.0*, Rigaku and Rigaku/MSC, The Woodlands, TX, 2000.
- 33 L. J. Farrugia, *J. Appl. Crystallogr.*, 1999, **32**, 837–838.
- 34 C. Kabuto, S. Akine, T. Nemoto and E. Kwon, *J. Cryst. Soc. Jpn.*, 2009, **51**, 218–224.
- 35 P. van der Sluis and A. L. Spek, *Acta Crystallogr.*, 1990, **A46**, 194–201.
- 36 I. D. Brown and D. Altermatt, *Acta Crystallogr.*, 1985, **B41**, 244–247.

Submitted to *Catal. Sci. Technol.* as an Article (revised)


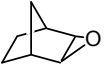
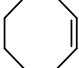

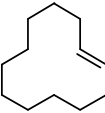
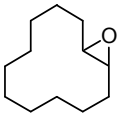
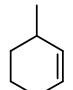
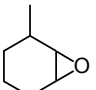
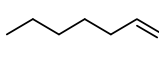
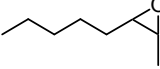
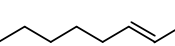
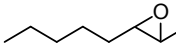
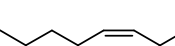
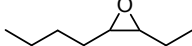
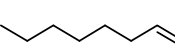
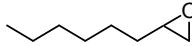
Table 1 Effects of catalysts on epoxidation of cyclooctene with H₂O₂^a

Entry	Catalyst (μmol)	Temp. (K)	Time (h)	Yield (%)
1	None	323	3	<1
2	I (4)	305	1	97
3	I (4)	273	5	90
4 ^b	I (4)	305	3.5	94
5	I (1)	305	3.5	94
6	PW10 (8)	305	1	12
7	TiO(acac) ₂ (16)	305	1	4
8	PW10 (8) + TiO(acac) ₂ (16)	305	1	94

^a Reaction conditions: Cyclooctene (5 mmol), 30% H₂O₂ (1 mmol), CH₃CN (6 mL).

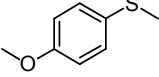
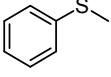
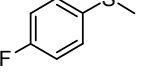
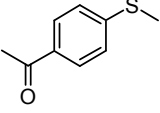
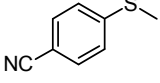
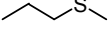
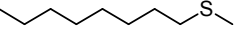
^b Cyclooctene (1 mmol). Yields were determined by GC with an internal standard. Yield (%) = epoxide (mol)/initial H₂O₂ (mol) \times 100.

Submitted to *Catal. Sci. Technol.* as an Article (revised)**Table 2** Epoxidation of various alkenes with H₂O₂ catalyzed by **I**^a

Entry	Substrate	Product	Time (h)	Yield (%)
1			3	75 (only <i>exo</i>)
2			1	97
3 ^b			2	90 (<i>cis/trans</i> = 12/88)
4			1	80 (<i>cis/trans</i> = 23/77)
5			5	82
6 ^c			9	43
7			3	70
8 ^c			8	54

^a Reaction conditions: **I** (4 μmol), substrate (5 mmol), 30% H₂O₂ (1 mmol), CH₃CN (6 mL), 305 K. ^b Substrate: *cis/trans* = 30/70. ^c 323 K. Yields were determined by GC with an internal standard. Yield (%) = epoxide (mol)/initial H₂O₂ (mol) × 100.

Submitted to *Catal. Sci. Technol.* as an Article (revised)**Table 3** Oxygenation of various sulfides with H₂O₂ catalyzed by **I**^a

Entry	Substrate	Time (min)	Yield (%)	
			Sulfoxide/sulfone	Total yield (%)
1		5	62/18	98
2		10	87/6	>99
3		10	88/6	>99
4		5	65/14	93
5		10	86/5	97
6		5	49/25	>99
7		5	55/18	90

^a Reaction conditions: **I** (2 μmol), substrate (1 mmol), 30% H₂O₂ (0.2 mmol), CH₃CN (1 mL), 305 K. Yields were determined by GC with an internal standard. Yield (%) = sulfoxide or sulfone (mol)/initial H₂O₂ (mol) × 100. Total yield (%) = {sulfoxide (mol) + sulfone (mol) × 2}/initial H₂O₂ (mol) × 100.

Submitted to *Catal. Sci. Technol.* as an Article (revised)

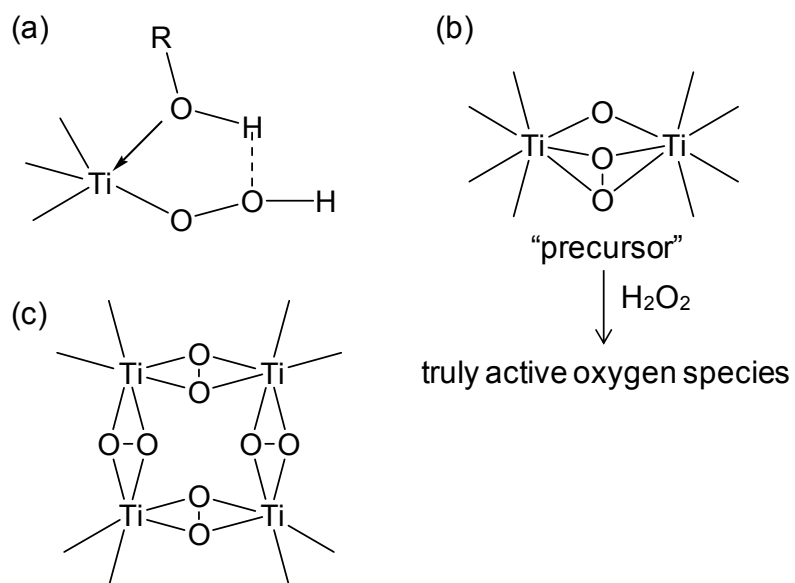


Fig. 1 (a) One of the postulated active oxygen species formed on TS-1,² (b) μ -oxo- μ - η^2 : η^2 -peroxo core in the Katsuki's Ti(salan) complex,^{3c} and (c) tetra- μ - η^2 : η^2 -peroxo core in **II** (this work).

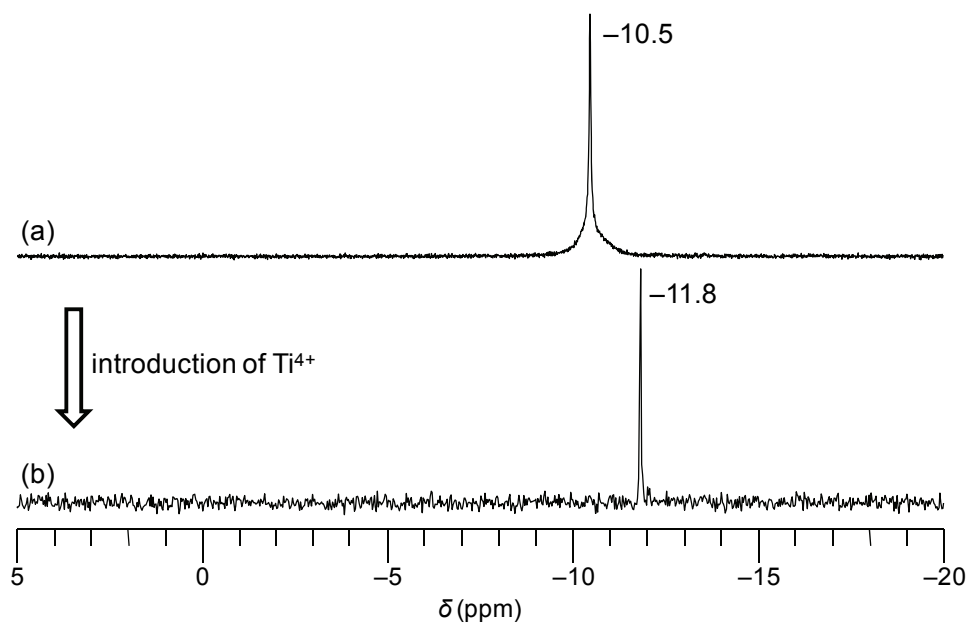
Submitted to *Catal. Sci. Technol.* as an Article (revised)

Fig. 2 ^{31}P NMR spectra of (a) PW10 in $\text{DMSO-}d_6$ and (b) **I** in CD_3CN .

Submitted to *Catal. Sci. Technol.* as an Article (revised)

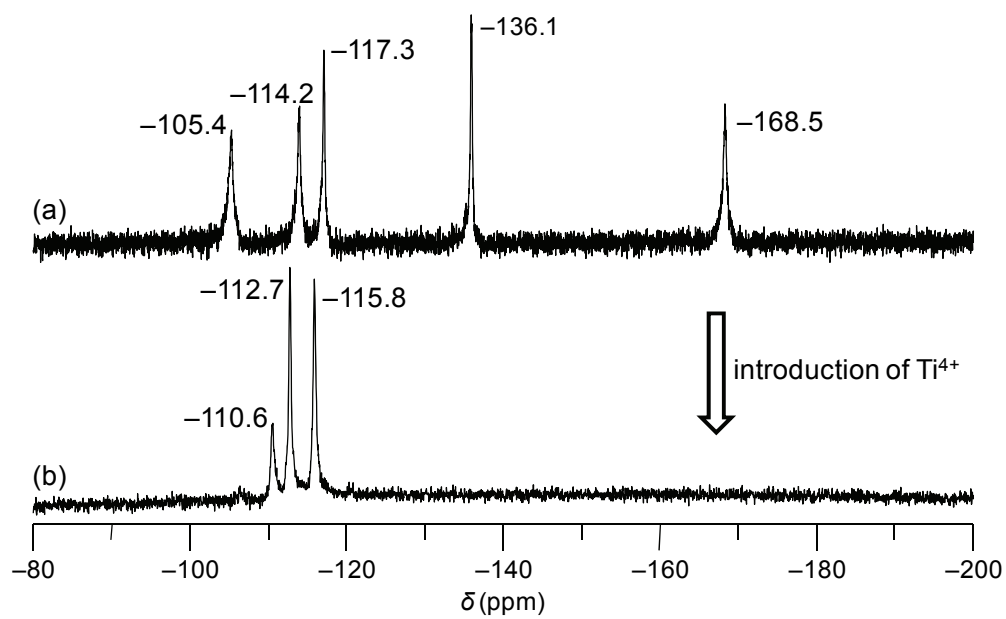


Fig. 3 ^{183}W NMR spectra of (a) PW10 in $\text{DMSO-}d_6$ and (b) **I** in $\text{CD}_3\text{CN/PC}$ (1:1 v/v).

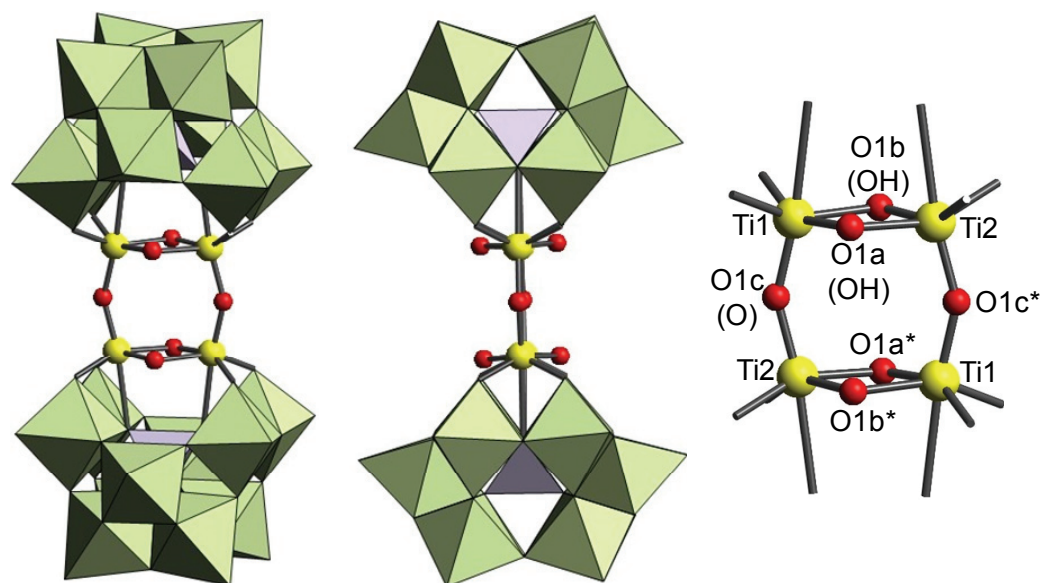
Submitted to *Catal. Sci. Technol.* as an Article (revised)

Fig. 4 Polyhedral and ball-and-stick representation of the anion part of **I**. The $\{\text{WO}_6\}$ and $\{\text{PO}_4\}$ units are shown as green octahedra and purple tetrahedra, respectively. Yellow and red spheres show Ti and O atoms, respectively.

Submitted to *Catal. Sci. Technol.* as an Article (revised)

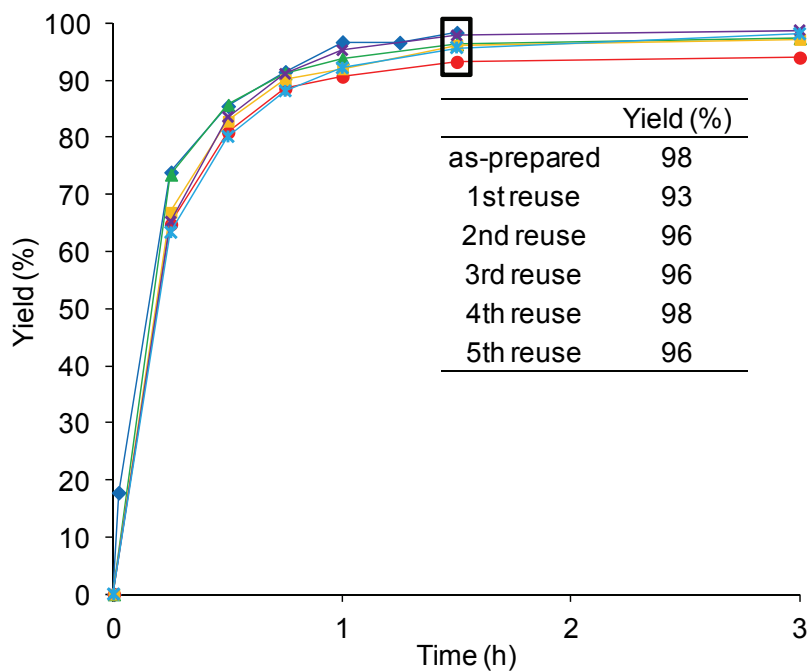


Fig. 5 Reuse experiments for the epoxidation of cyclooctene with H_2O_2 ; the profiles for **I** (blue diamond), and the first (red circle), second (green triangle), third (yellow square), fourth (purple cross), and fifth (blue asterisk) reuse experiments. Reaction conditions: **I** ($4 \mu\text{mol}$), cyclooctene (5 mmol), $30\% \text{ H}_2\text{O}_2$ (1 mmol), CH_3CN (6 mL), 305 K .

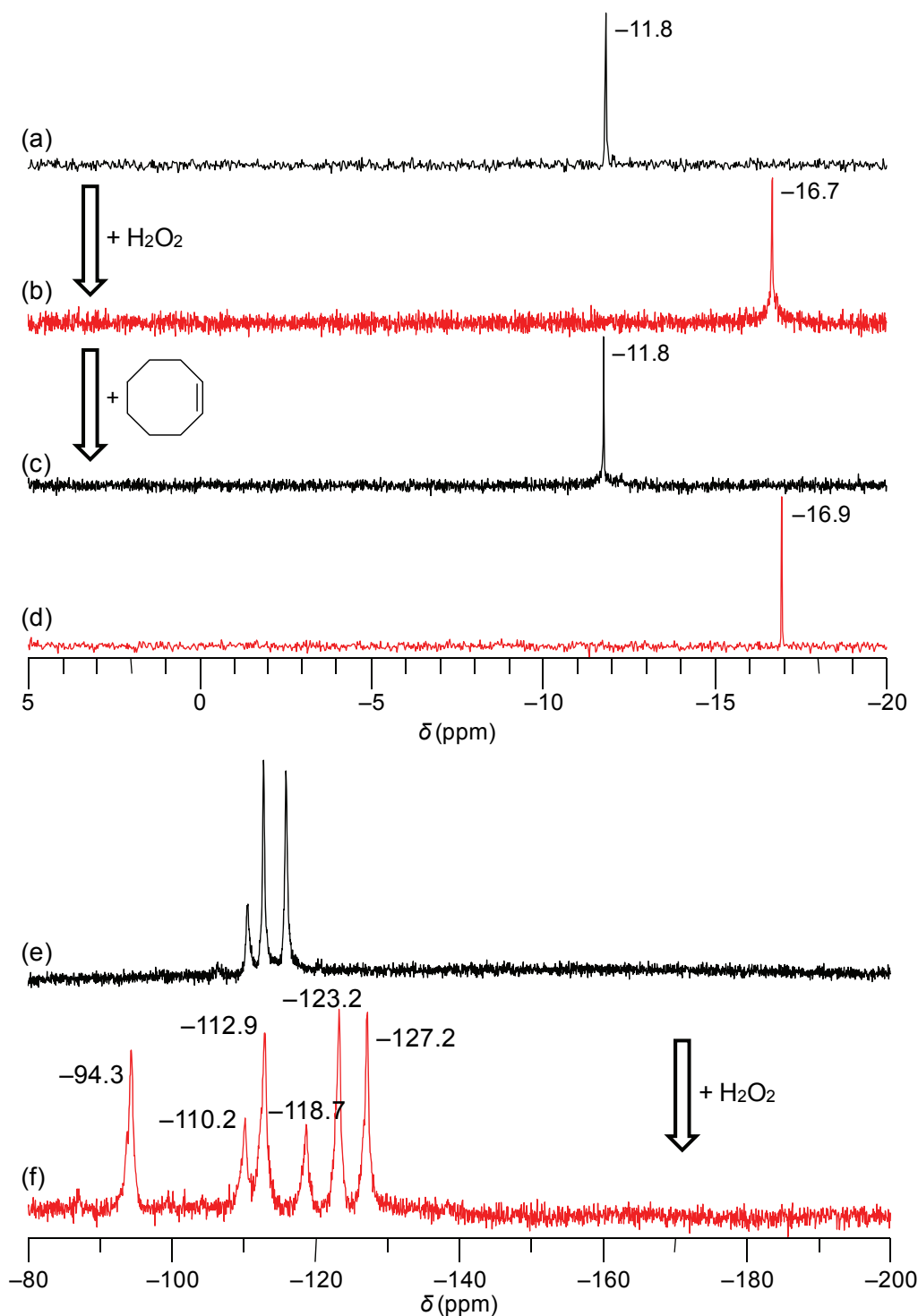
Submitted to *Catal. Sci. Technol.* as an Article (revised)

Fig. 6 ^{31}P NMR spectra of (a) **I**, (b) in-situ-formed **II** (**I** + 128 H_2O_2), (c) in-situ-formed **II** + 128 equivalents of cyclooctene, and (d) isolated single crystals of **II** in CD_3CN ; ^{183}W NMR spectrum of (e) **I** and (f) in-situ-formed **II** (**I** + 64 H_2O_2) in $\text{CD}_3\text{CN}/\text{PC}$ (1:1 v/v).

Submitted to *Catal. Sci. Technol.* as an Article (revised)

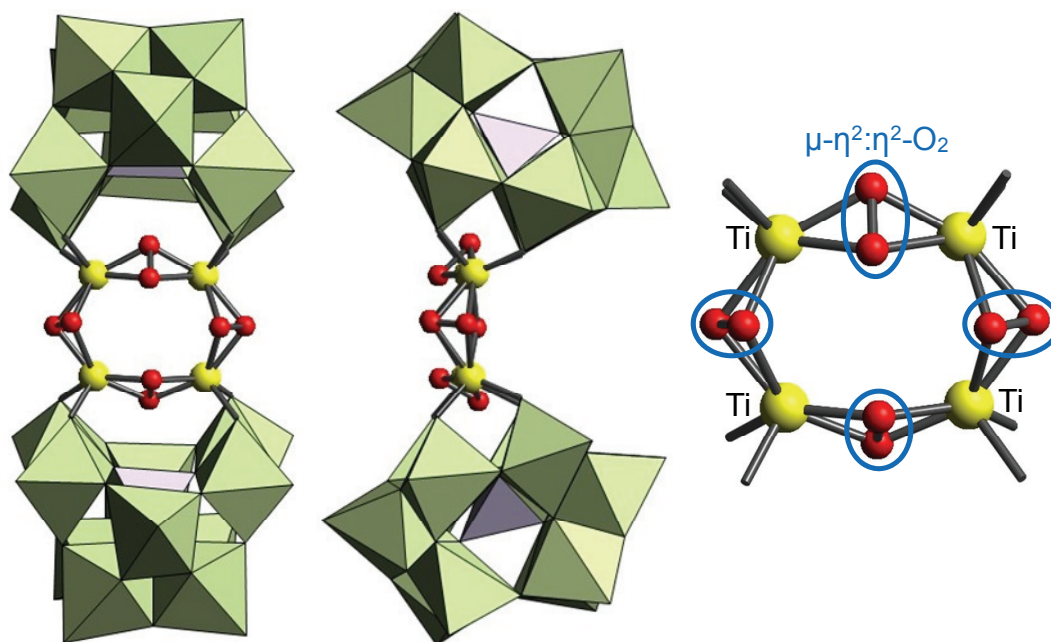
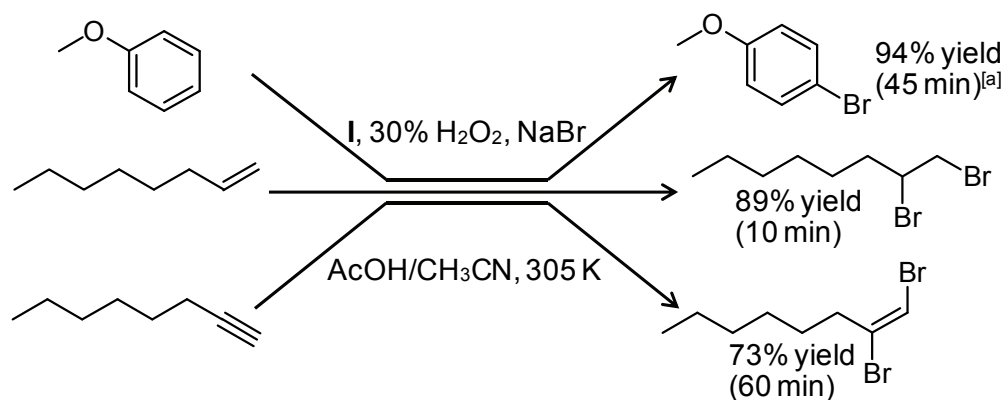
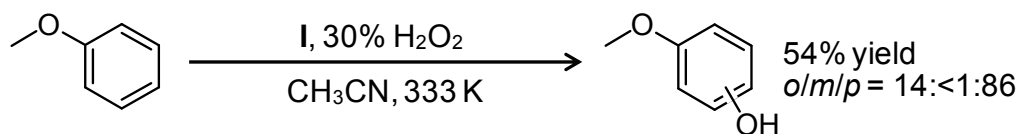


Fig. 7 Polyhedral and ball-and-stick representation of the anion part of **II**. The {WO₆} and {PO₄} units are shown as green octahedra and purple tetrahedra, respectively. Yellow and red spheres show Ti and O atoms, respectively.

Submitted to *Catal. Sci. Technol.* as an Article (revised)

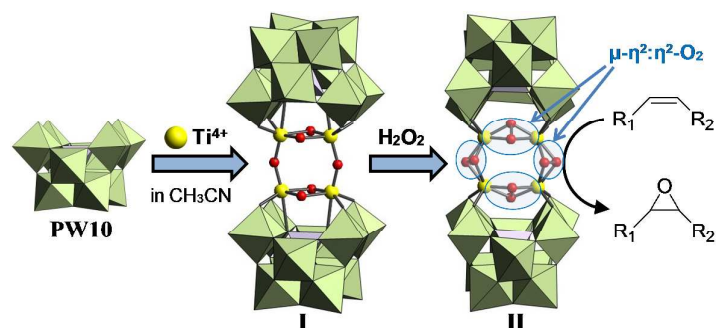
Scheme 1 Oxidative bromination of unsaturated compounds with H₂O₂ catalyzed by **I**. Reaction conditions: **I** (0.25 μmol), substrate (1 mmol), NaBr (2 mmol), 30% H₂O₂ (1 mmol), AcOH/CH₃CN (2/1 mL), 305 K. [a] NaBr (1 mmol). Yields were determined by GC with an internal standard. Yield (%) = product (mol)/initial H₂O₂ (mol) × 100.

Submitted to *Catal. Sci. Technol.* as an Article (revised)



Scheme 2. Hydroxylation of anisole with H₂O₂ catalyzed by **I**. Reaction conditions: **I** (1.25 μmol), anisole (5 mmol), 30% H₂O₂ (0.1 mmol), CH₃CN (2 mL), 333 K, 120 min. Yields were determined by GC with an internal standard. Yield (%) = product (mol)/initial H₂O₂ (mol) × 100.

Graphical abstract



A Ti-substituted phosphotungstate (**I**) showed high catalytic performance for several oxidation reactions. The truly catalytically active species was successfully isolated, and its anion structure was determined.